CHAPTER 8
COMPUTATIONAL ANALYSIS OF MULTIDIMENSIONAL FLOW

M.B. Carver
Atomic Energy of Canada Limited
Chalk River Nuclear Laboratories
Chalk River, Ontario, Canada K0J 1J0

ABSTRACT

Components of the reactor system are identified in which multidimensional computational thermalhydraulics can be used to advantage. Models of single- and two-phase flow are reviewed. Suitable computational algorithms are introduced briefly and some example applications are given.

1.0 INTRODUCTION

As a nuclear reactor system relies entirely on fluid circuits for energy transport, mathematical modelling of thermalhydraulic phenomena plays an important role in reactor design and development, and methods of improving the accuracy and efficiency of thermalhydraulic computations are sought continually. A simplified fluid circuit diagram of a CANDU reactor is shown in Figure 1. Throughout most of the piping network, the fluid behaviour may be adequately described by one-dimensional (cross-sectional averaged) models such as those described earlier. However, in the reactor fuel channel, flow must distribute itself amongst the intricate flow passages of the fuel bundle. In the secondary side of the steam generator, and in the calandria, the flow distribution is also complex. One-dimensional analysis is adequate to simulate overall or bulk energy transfer, but multi-dimensional analysis is necessary to model detailed local distribution of flows and temperatures in any of these gometrically complex components. It is interesting to note that all these components have a similar internal structure, that is, flow passes through some form of rod or tube array.

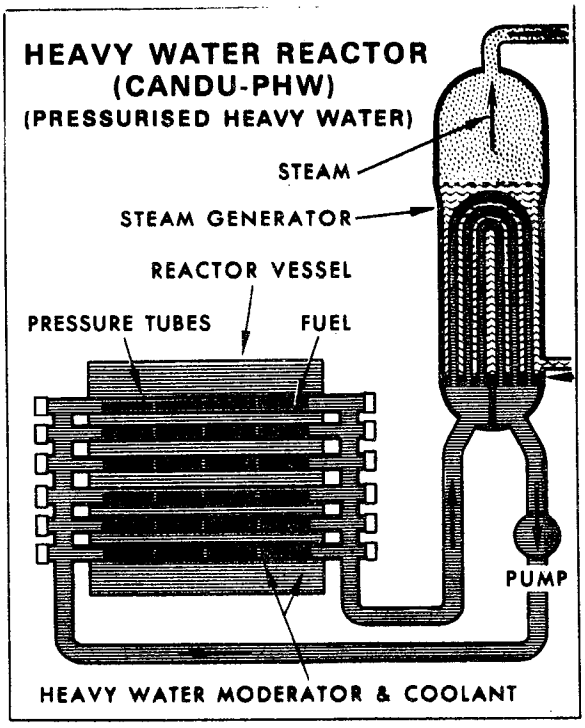

Figure 1. Simplified View of CANDU Reactor

2.0 MODELS OF SINGLE-PHASE FLOW

The first step in any computation is to decide on a flow model. The most complicated available model need normally not be used; simplifying assumptions are frequently valid and may reduce the complexity of the equations to be solved.

Single-phase flow is normally modelled adequately by solving the conservation equations of mass, momentum, and energy. The exact form of the equations will depend first on whether the fluid should be considered incompressible or compressible and secondly whether the fluid should be considered inviscid or viscous. These decisions affect both the form of the equations and the behavioural modes of the solution.

The above considerations are common to single or multidimensional form. However, the problem of turbulence modelling is peculiar to multidimensional flow modelling. The model of turbulence exerts influence only by means of its effects on pressure drop in a 1D calculation, but it determines velocity distribution in two and three dimensions. It is usually modelled by effective viscosity[1)] and a suitable means of computing the distribution of effective viscosity is sought. This may be introduced by algebraic relationships or the more detailed models involving further differential equations of transport. It should be emphasized that additional differential equations thus introduced are not governing equations of the flow field but merely part of the turbulent model.

Frequently in incompressible flow, the energy equation is decoupled from the flow field solution by using the Boussinesq approximation[2]. This considers the density field to be invariant throughout the equations. Buoyancy effects are then approximated by making the density in the momentum equation gravity term only a function of temperature.

3.0 GEOMETRIC FRAMEWORK

A model of the geometries required as a framework for the analysis. The form is often dictated by the hardware. Alternative computational frameworks for rod array systems are received by Shah[3].

Although the finite element method lends itself readily to fitting complex external boundaries, it has not often been used for systems with complex internal boundaries. Instead the equations have usually been formulated for finite control volumes and integrated in finite difference form.

Except for the 1D case, the simplest and most natural geometric division of a rod array is by subchannel. Subchannels are readily defined as communicating flow channels bounded by rod surfaces, and fictitious lines between rod centres. Each subchannel is divided into number of axial control volumes.

An alternative approach is to impose an orthogonal coordinate system on the entire flow vessel and represent the internal hardware by distributed resistances and heat sources. This classic 'porous medium' approach is more suitable for geometries in which rods are densely packed and information on overall flow distribution inside the rod array is required rather than details of each individual subchannel. Here porosities are assigned as the fraction of each control volume available to the fluid, i.e., not occupied by hardware, and flow area blockages are computed by suitably averaging at control volume interfaces.

A more precise procedure is to assign true values of area blockages at control volumes faces rather than approximate them by averaging. This permits a more accurate representation of geometries like fuel bundles in which the control volumes chosen do not contain several rods, but may in fact contain few rods, a partial rod or none at all[4].

In either form, however, the porosity concept is still an artifact; it does not reduce to the true solution in the limit as zero velocity cannot be imposed at all solid surfaces. In fact, standard finite element methods do not so reduce either. This degree of fidelity can be achieved only by using finely divided body fitted coordinates[3].

The examples in this paper are restricted to the subchannel and porous medium formulations. Some of their features are summarized in Figure 2.

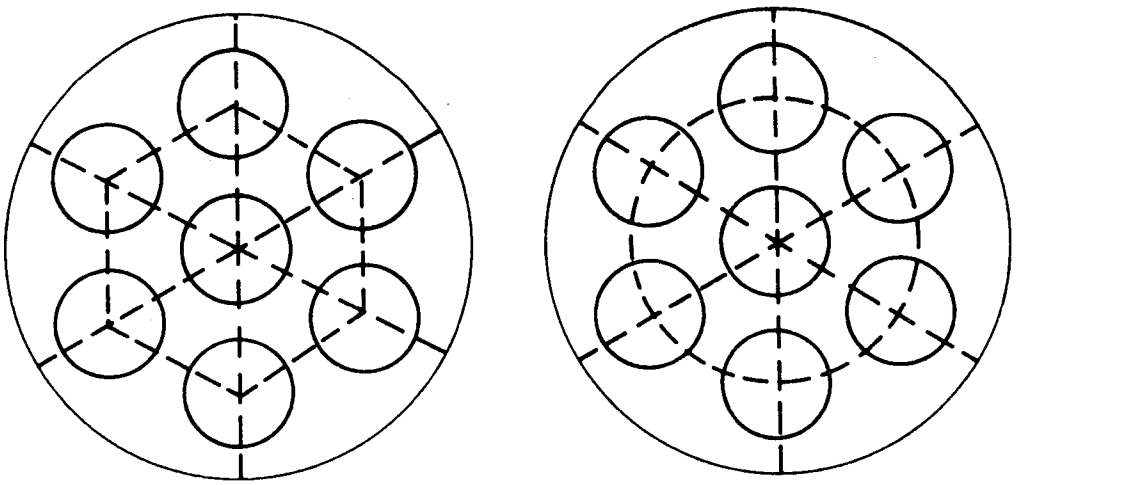

Figure 2. Geometric Framework for Rod Bundles

4.0 SOLUTION OF THE SINGLE-PHASE FLOW EQUATIONS

4.1 Statement of the Equations

The differential equations of mass, momentum and energy are expressed for each particular control volume and are to be solved for all control volumes. In one-dimensional analyses, solutions are frequently obtained simultaneously for all flow variables throughout the field. However, equation systems resulting from multidimensional analyses are too large to permit simultaneous solution and some form of segmentation of the problem is required with iteration to merge the segments.

4.2 Reduction to Discretized Form

The conservation equations are given in detail in Table 1. In order to solve the equations it is necessary to write them in discrete form with reference to finite control volumes. To maintain continuous definition of all variables it is important that all variables are evaluated correctly

TABLE 1

Conservation Equations for Three Dimensional Analysis of a Single or Homogeneous Two-Phase Flow Field, including terms catering for transients, porosity, turbulent viscosity and compressibility

Continuity

$$\frac{\partial}{\partial t}(\beta\rho) + \frac{\partial}{\partial x}(\beta\rho u) + \frac{1}{r}\frac{\partial}{\partial r}(\beta\rho r v) + \frac{1}{r}\frac{\partial}{\partial \theta}(\beta\rho w) = 0$$

Axial Momentum

$$\frac{\partial}{\partial t}(\beta\rho u) + \frac{\partial}{\partial x}(\beta\rho u^2) + \frac{1}{r}\frac{\partial}{\partial r}(\beta\rho r v u) + \frac{1}{r}\frac{\partial}{\partial \theta}(\beta\rho w u) + \beta\left(\frac{\partial p}{\partial x} + \rho g_x + f_x\right)$$
$$= \frac{\partial}{\partial x}\left(\beta\mu_t \frac{\partial u}{\partial x}\right) + \frac{1}{r}\frac{\partial}{\partial r}\left(\beta\mu_t r \frac{\partial u}{\partial r}\right) + \frac{1}{r}\frac{\partial}{\partial \theta}\left(\frac{\beta\mu_t}{r}\frac{\partial u}{\partial \theta}\right)$$

Radial Momentum

$$\frac{\partial}{\partial t}(\beta\rho v) + \frac{\partial}{\partial x}(\beta\rho u v) + \frac{1}{r}\frac{\partial}{\partial r}(\beta\rho r v^2) + \frac{1}{r}\frac{\partial}{\partial \theta}(\beta\rho v w) + \beta\left(\frac{\partial p}{\partial r} + \rho g_r + f_r - \rho\frac{w^2}{r}\right)$$
$$= \frac{\partial}{\partial x}\left(\beta\mu_t \frac{\partial v}{\partial x}\right) + \frac{1}{r}\frac{\partial}{\partial r}\left(\beta\mu_t r \frac{\partial v}{\partial r}\right) + \frac{1}{r}\frac{\partial}{\partial \theta}\left(\frac{\beta\mu_t}{r}\frac{\partial v}{\partial \theta}\right)$$

Tangential Momentum

$$\frac{\partial}{\partial t}(\beta\rho w) + \frac{\partial}{\partial x}(\beta\rho u w) + \frac{1}{r}\frac{\partial}{\partial r}(\beta\rho v w) + \frac{1}{r}\frac{\partial}{\partial \theta}(\beta\rho w^2) + \beta\left(\frac{1}{r}\frac{\partial p}{\partial \theta} + \rho g_\theta + f_\theta + \rho\frac{vw}{r}\right)$$
$$= \frac{\partial}{\partial x}\left(\beta\mu_t \frac{\partial w}{\partial x}\right) + \frac{1}{r}\frac{\partial}{\partial r}\left(\beta\mu_t r \frac{\partial w}{\partial r}\right) + \frac{1}{r}\frac{\partial}{\partial \theta}\left(\frac{\beta\mu_t}{r}\frac{\partial w}{\partial \theta}\right)$$

Energy

$$\frac{\partial}{\partial t}(\beta\rho h) + \frac{\partial}{\partial x}(\beta\rho u h) + \frac{1}{r}\frac{\partial}{\partial r}(\beta\rho r v h) + \frac{1}{r}\frac{\partial}{\partial \theta}(\beta\rho w h)$$
$$= s_h^* + \frac{\partial}{\partial x}\left(\beta\Gamma_t \frac{\partial h}{\partial x}\right) + \frac{1}{r}\frac{\partial}{\partial r}\left(\beta r\Gamma_t \frac{\partial h}{\partial r}\right) + \frac{1}{r}\frac{\partial}{\partial \theta}\left(\frac{\beta\Gamma_t}{r}\frac{\partial h}{\partial \theta}\right)$$

State

$$\rho = \rho(h, p)$$

Nomenclature

The equations are written in cylindrical coordinates. To convert to cartesian, substitute $r = 1$, $\frac{\partial}{\partial r} = \frac{\partial}{\partial y}$, $\frac{\partial}{\partial \theta} = \frac{\partial}{\partial x}$.

u, v, w are velocity components in x, r, θ

ρ, h, p are density, enthalpy and pressure

μ_t^*, Γ_t^* are effective viscosity and diffusivity

β is porosity

g_x, g_r, g_θ, f_x^*, f_r^*, f_θ^* are x, r, θ components of gravity and friction losses

* denotes constitutive relationships are required

where averages across grid points are required. The concept of staggered grid facilitates this. Scalar variables such as pressure, density and enthalpy are stored at primary node points, whereas velocities are considered to act between pressures as shown in Figure 3. The momentum equations are thus written for control volumes centered on velocities, whereas the continuity and energy equations are centered on the primary nodes.

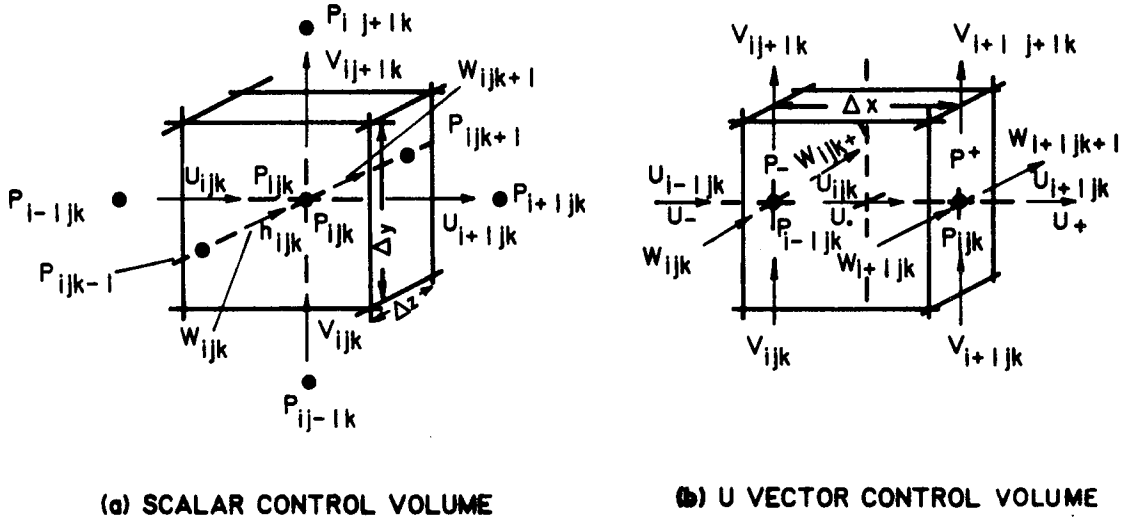

(a) SCALAR CONTROL VOLUME (b) U VECTOR CONTROL VOLUME

Figure 3. Staggered mesh for Three Dimensional Computation

Most common schemes for multidimensional flow originate from one of two major sources, the ICE[5] procedures developed at LASL and the SIMPLE[6] procedures from Imperial College. Both use the staggered grid concept, although the nomenclature is somewhat different, and the ICE procedures solve the equations in differential form, whereas SIMPLE disciples prefer to integrate about the control volume. Both apply equally well to 1, 2 and 3D situations. The 1D momentum equation is used as an example of each philosophy in Table 2. It is apparent that the resulting equations are equivalent.

4.3 Solution of the Equation Set

The resulting equation set has four primary variables: velocity (three components), density, enthalpy and pressure. These are linked by three conservation equations and the equation of state (neglecting viscosity for the moment).

It is convenient for illustration purposes to now write the continuity and momentum equations from Table 1 in simplified form using vector notation.

TABLE 2

Discretization of Simplified Momentum Equation

$$\frac{\partial}{\partial t}(\rho u) + \frac{\partial}{\partial x}(\rho u^2) + \frac{\partial p}{\partial x} + \rho g_x + f_x = 0$$

SIMPLE Notation u_i is upstream in x from p_i

Integrate over volume VOL = $\int A(x)dx = \bar{A}\delta x$

$$\left[\frac{VOL}{\delta t}\bar{\rho}_{i1-1} + A_i\rho_i\,\bar{u}_{i1+1}\right]u_i = \left[A_{i-1}\,\rho_{i-1}\,\bar{u}_{i1-1}\right]u_{i-1}$$
$$- \bar{A}_{i1-1}(p_i - p_{i-1}) + \bar{\rho}_{i1-1}\,u^o\,\frac{VOL}{\delta t} - VOL\left[\bar{\rho}_{i1-1} + f_{x_{u_i}}\right]$$

ICE Notation u upstream in x from p_i is denoted $u_{i-\frac{1}{2}}$

$$\frac{(\bar{\rho}u)_{i-\frac{1}{2}}}{\delta t} = \frac{(\bar{\rho}u)^o_{i-\frac{1}{2}}}{\delta t} + \frac{A_{i-1}(\bar{\rho}u^2)^o_{i-\frac{1}{2}}}{\delta x} - \frac{A_i(\rho u^2)^o_{i+\frac{1}{2}}}{\delta x}$$
$$- \bar{A}_{i-\frac{1}{2}}(p_i - p_{i-1}) - \bar{\rho}^o_{i-\frac{1}{2}}\,g_x - f^o_{x_{u_{i-\frac{1}{2}}}}$$

In the SIMPLE procedure, all the terms except u^o are at new time. In the ICE procedure only the u term and pressure terms are at new time.

$$\frac{\partial}{\partial t}(\beta\rho) + \frac{\partial}{\partial x_j}(\beta\rho u_j) = 0 \qquad \ldots \quad (1)$$

$$\frac{\partial}{\partial t}(\beta\rho u_i) + \frac{\partial}{\partial x_j}(\beta\rho u_i u_j) = -\left[\frac{\partial P}{\partial x_i} + \rho g_i + \Gamma_i\right]\beta \qquad \ldots \quad (2)$$

Here v_i denotes the velocity component along x_i,

$$\frac{\partial u_j}{\partial x_j} = \frac{\partial u}{\partial x} + \frac{\partial v}{\partial y} + \frac{\partial w}{\partial z},$$

Γ_i contains friction centrifugal and viscous terms and 100% porosity is assumed.

Equation can now be discretized with reference to the control volume in Figure 3.

$$\frac{(\beta\rho u)_i - (\beta\rho u)^0_i}{\Delta t} + \sum_j \frac{(\beta\rho u_i u_j)_+ - (\beta\rho u_i u_j)_-}{\Delta x_j} + \frac{\beta(P_+ - P_-)}{\Delta x_i} = S_{m_i} \qquad \ldots \quad (3)$$

Both the SIMPLE and ICE schemes are based on solving the momentum equations for a first estimate of each velocity component, and also extracting a pressure equation from continuity considerations. In general, each momentum equation is reduced by appropriate discretization, integration and linearization to an algebraic equation, which can be written

$$[a_m(\rho u)_m = \sum_n a_n(\rho u)_m + b(P_+ - P_-) + c]_i \quad i = 1,3 \qquad \ldots \quad (4)$$

This links the mass flux component (ρu) at the point m to neighbouring mass fluxes in all directions, and to the pressure gradient in the i direction. Similarly, the continuity equation can be reduced to a discrete form

$$\frac{\partial \rho}{\partial t} - \sum_i e_i(\rho u_{in} - \rho u_{out}) = D \approx 0 \qquad \ldots \quad (5)$$

The coefficients a in (4) absorb the nonlinearity of the momentum equations, coefficients a and c may incorporate transient terms, e is the area available to the fluid at the appropriate control volume face.

First estimates of each velocity component u_m may be obtained by solving equations (4) using an assumed pressure field. When these are inserted in (5), however, the equation will not exactly balance but instead, compute a divergence D because of the nonlinearities and inaccuracies in the assumed pressure field. However, a new velocity field which will more closely fulfill continuity may be obtained by computing the pressure changes required to drive D to zero for the next iteration m+1. The Newton-Raphson technique establishes these to be

$$dP = P_{m+1} - P_m = \frac{D_{m+1} - D_m}{dD/dP} = \frac{-D}{dD/dP} \qquad \ldots \quad (6)$$

or

$$dD = \frac{dD}{dP}\, dP = -D \qquad \ldots \quad (7)$$

An expression for dD is readily determined by differentiating (5)

$$\frac{dD}{dP} = \frac{1}{\delta t}\frac{d\rho}{dP} - \sum_i e_i \left[\frac{d(\rho u)_{in}}{dP} - \frac{d(\rho u)_{out}}{dP}\right]_i = -D \qquad \ldots \quad (8)$$

by differentiating (4) and simplifying,

$$\left[d(\rho u)_m\right]_i = \left[b(dP_+ - dP_-)_m\right]_i \qquad \ldots \quad (9)$$

Combining (8) and (9) gives a matrix equation for the pressure change field, which can be written in general form

$$q_m dP_m = \sum q_n dP_n - D \qquad \ldots \quad (10)$$

Equation (9) can be used to solve for the required pressure change field, which in turn is applied to correct the velocities according to equation (10). The entire process must be iterated to converge through the nonlinearities.

It is useful to note that equations (9) and (10), and in fact most other relevant transport equations, can be written in a general form

$$a_m \phi_m - \sum_n a_n \phi_n = S \qquad \ldots \quad (11)$$

This is a general matrix equation which relates a variable ϕ at the point m to its neighbours at points n. All other variables are collected in the source term, S. Thus the same matrix algorithm may be used to solve all such equations. Equation (11) can be one-, two- or three-dimensional. Direct solutions are expensive, so inner iteration may be used to solve (11). Iteration is all the more economical, as (11) itself need not be iterated to converge as the whole process (4) to (10) is repeated.

The above sequence is the foundation of the flow field solution. In single-phase flow the energy equation is not closely coupled. It can be reduced to the form of equation (11) and solved subsequently to the flow field. The equation of state is then used to determine the density field or the Boussinesq term and the viscosity field may also be computed. The iteration is then repeated from equation (1) using the new density, viscosity and pressure fields until all fields converge.

The sequences above assume an elliptic flow field in which all boundary conditions are known and the equations are solved simultaneously throughout the field for the primary variable of each segment. In duct flows with a linear axial pressure gradient the field may be assumed to be parabolic. Entry values are known and the solution is marched downstream using a two-dimensional elliptic step in each axial plane. For curved ducts, or ducts with resistances, downstream conditions do influence the flow upstream, so partially parabolic sequences may be used to iterate over the marching sequence. These variations are reviewed by Patankar[7].

5.0 A SINGLE-PHASE EXAMPLE - MODERATOR FLOW CIRCULATION IN A REACTOR CALANDRIA

The example simulates flow in the moderator using a 2D application of the SIMPLE technique[8]. A turbulence model and a finely divided grid was required to simulate the entrainment of flow in the neighbourhood of injector nozzles, and the volumetric porosity concept was used to simulate the pressure tube array. The model was compared with an adiabatic experiment, and then extended to diabatic reactor conditions. This work is described fully in reference 8. The illustration used here in Figure 4 is the adiabatic comparison from reference 8 showing agreement between the computed and measured velocity fields.

Moderator flow has also been simulated in 3D[9]. Because the study was in 3D it had to use a coarser grid. It did not incorporate a turbulence model.

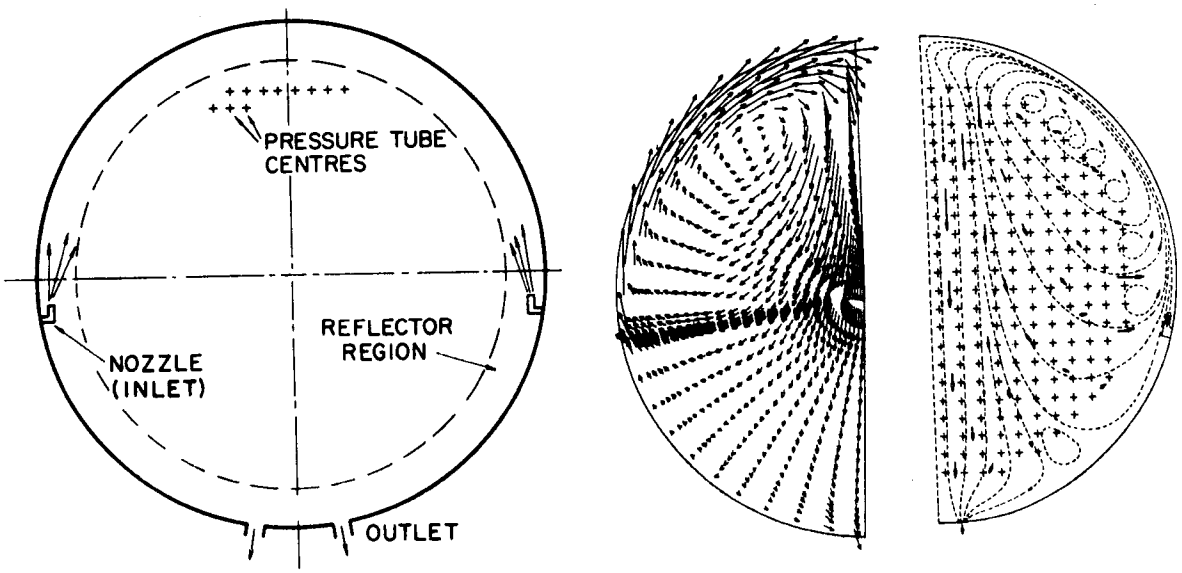

Figure 4. Moderator Simulation

(a) Simplified Front View of Typical 600 MW Calandria Vessel
Pickering Isothermal Experiments
(b) Predicted Velocity Field using a 34 x 30 grid, and
(c) Measured Velocity Field

6.0 MODELS OF TWO-PHASE FLOW

The assumption of equilibrium produces the simplest model in which the phases are taken to be homogeneously mixed, and to have equal velocity and equal temperature, hence the terminology EVET model. The two-phase mixture is treated as a single fictitious fluid having properties determined solely by the relative proportion by weight (quality) of vapour in the mixture. Thus the partial differential equations to be solved are the same as for single-phase flow: conservation of mass, momentum and energy of the mixture; algebraic relationships cater for the two-phase properties and the equation of state for the mixture. The homogeneous model is suitable for conditions in which departures from mechanical and thermal equilibrium are known to be minimal.

For cases in which gravitational or centrifugal forces are known to produce a tendency for phases to travel at different speeds, a two-velocity model is required, and an additional relationship is required for relative velocity. Early separated flow models used void correlation instead of the equation of state and a simple numeric slip factor to impose the higher velocity of the vapour phase in vertical flow. This was later quantified by relating relative velocity to the rise velocity of vapour bubbles in liquid and radial distribution of vapour under various conditions. This simple drift flux model, also referred to as DF-ET, unequal velocity equal temperature, uses algebraic relationship for relative velocity, and hence still requires the solution of the same three partial differential equations of conservation, but an additional equation, usually based on gaseous phase continuity, is required for void distribution.

None of the above models permits the temperature of either phase to depart from saturation. In order to simulate non-equilibrium phenomena such as subcooled boiling, superheated liquid and flashing, etc., a mechanism which permits these effects must be added. Again, early studies used algebraic relationships, but more rigorous models now use a separate energy equation, and equation of state for each phase and model heat transfer to and between phases. The EVUT model is, therefore, also a four equation model.

The 'advanced drift flux' DF-UT model is a combination of both of the above, and, therefore, requires the solution of five conservation equations, a mixture momentum equation, two continuity equations and two energy equations.

Finally, the full six equation, two-fluid model or UVUT abandons the algebraic definite of relative velocity and instead computes phase velocities using two momentum equations containing models of wall to fluid and fluid to fluid stresses.

It is apparent that with each level of complexity of the two-phase model, additional partial differential equations are added, and hence more involved numerical schemes are required.

7.0 EXAMPLE OF MULTIDIMENSIONAL ANALYSIS OF TWO-PHASE FLOW

7.1 A Homogeneous Model Example - Secondary Side Flow in a Steam Generator

An example of the application of multidimensional modelling of two-phase flow is the analysis of secondary fluid flow in steam generators such as the one shown in Figure 5. The secondary fluid flows up through a fairly dense matrix of tubes which contain the primary fluid flow. The tube matrix provides high frictional resistance and heat transfer. These yield large source terms in the equations which tend to dominate the computation. Thus the iterative method tends to converge quite readily. Figure 5 also shows typical flow fields computed by the THIRST code, a program for multidimensional thermalhydraulic analysis of steam generators[10].

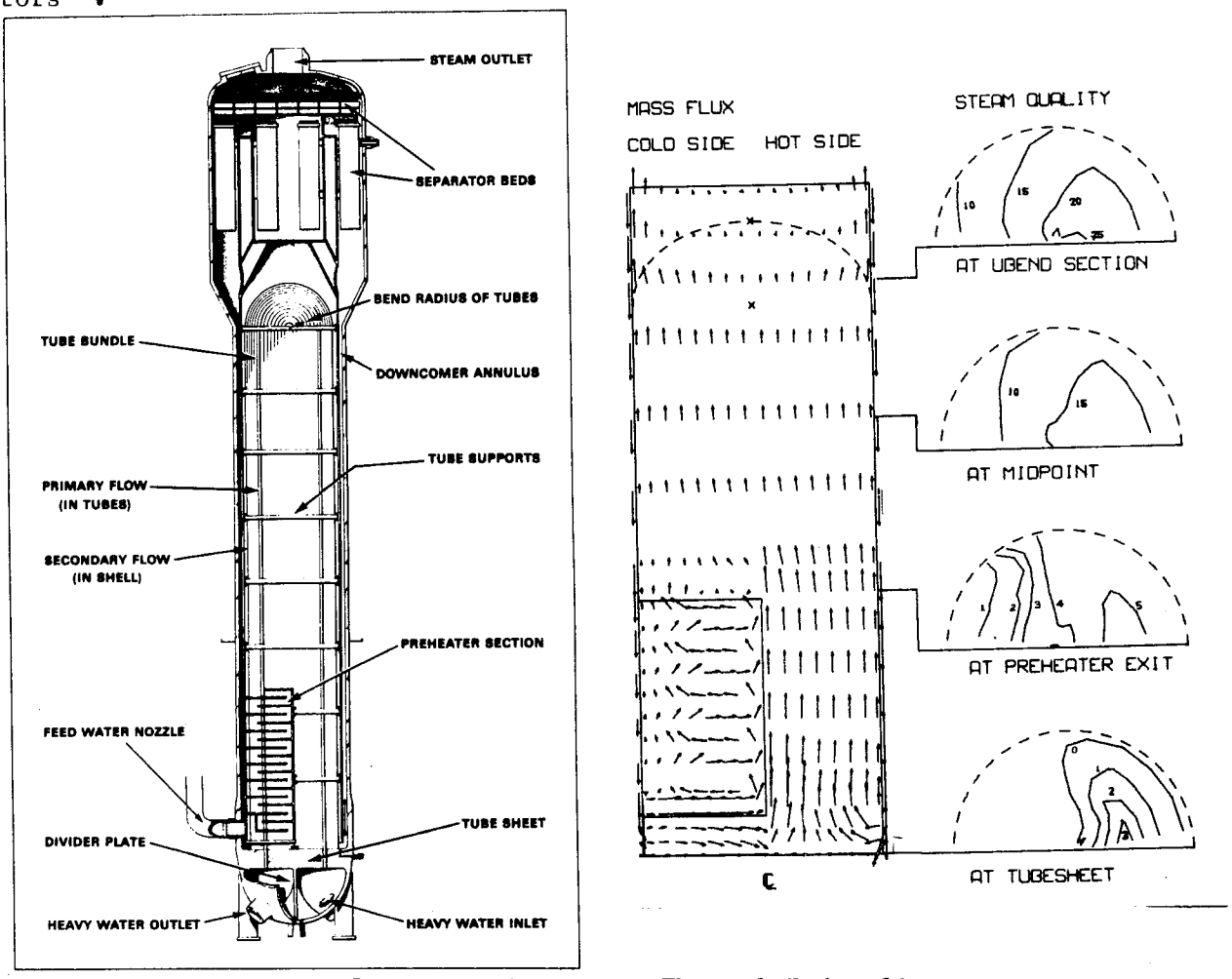

Figure 5. Steam Generator Thermal Hydraulics

(a) Cross Sectional View

(b) Computed Mass Flux and Quality Profiles

The left side of the figure is a vertical cut through the steam generator showing velocity profiles at each axial plane, while the right side shows steam quality distribution on selected axial planes.

7.2 A Basic Drift Flux Model Example - Two-Phase Flow in Horizontal Subchannels

The SAGA code[11] uses the basic drift flux model to compute two-phase flow in horizontal or vertical communicating channels. The numerical scheme is as outlined above except that the drift flux model is used to compute vapour cross flow from mixture cross flow. The vapour continuity equation is then used to correct the axial vapour velocities for cross flow, and all the mixture momentum equations are then assembled from separated flow form. The SAGA code can thus compute phase separation due to gravity. The code has been used to simulate the experiments of Tapucu in which two identical horizontal parallel channels were used. In experiment H_R^D-1, water enters the lower channel and an air/water mixture enters the upper channel. In experiment H_D^R-1 conditions are reversed, the air entering the lower channel. Figure 6 shows computed and measured void fraction profiles in the two channels. Full details of the SAGA code are given in the user's guide[11].

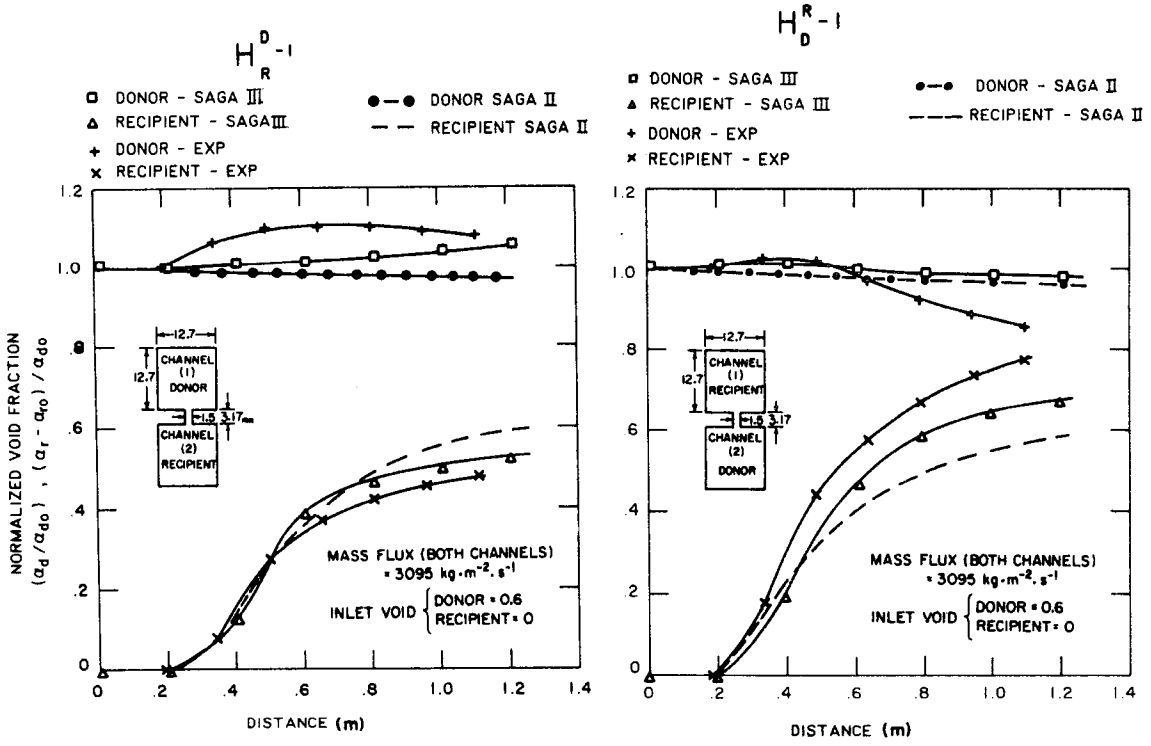

Figure 6. SAGA Code Simulation of Tapucu Experiments

7.3 Example of Advanced Drift Flux Model Applications - Two-Phase Flow in Horizontal Channels and Rod Bundles

The COBRA-IIIC subchannel code[13] has been used as a base from which to develop the code ASSERT (Advanced Solution of Subchannel Equations in Reactor Thermalhydraulics)[14]. This extends the SAGA drift flux model to include multiple subchannels and departure from saturation.

ASSERT has also been compared with the experiments of Tapucu[12]. Shown in Figure 7 are computed and measured distributions of pressure, void fraction and liquid mass flux in the two channels for experiment H_D^R-1, and a simplified sketch of the geometry. It is apparent that the high void or donor channel develops a higher inlet pressure drop. This causes an interesting exchange phenomenon. The lateral pressure gradient initially forces both liquid and vapour currently from the donor to the receiver. Eventually, however, gravity effects predominate, and counter-current cross flow is set up. Full details of these comparisons are given in reference 14.

As the goal of the ASSERT code development is the prediction of flow distribution in horizontal fuel bundles, a further example is included to illustrate that the model has progressed towards this goal.

Boiling water flow in a fictitious horizontal 7-rod bundle is simulated using the unequal velocity, unequal temperature model. The redistribution of flow due to end plates is modelled by local diffusion, otherwise turbulent exchange between channels is modelled as mentioned above. Heat input is assumed uniform. Typical volume fraction profiles are shown in Figure 8. Note that the gravity effect dispels thermalhydraulic symmetry, and subchannel 5, for example, assembles more steam than the geometrically similar subchannel 3. The end plates tend to redistribute the flow towards a more uniform distribution. No detailed experimental data on two-phase flow distribution are yet available, but such experiments are underway at CRNL and will provide a basis for code validation.

7.4 Examples of Two Fluid Model Computation Two-Phase Flow in Horizontal Channels and Vertical Elbows

The final examples are taken from the adiabatic 2D two-fluid code TOFFEA (Two Fluid Flow Equation Analyses)[15]. Again, the philosophy of the computation is the same, but two momentum equations and two continuity equations are used as summarized in Table 3. The gravitational and centrifugal forces tend to separate the fluids, the interphase drag terms counteract this tendency. Reference 15 gives details of the manner in which linear combinations of the continuity equations are assembled to derive the pressure equation and the additional equation from which void fraction is extracted.

The first application considered for illustration of the method is a comparison with the experiments of Gardner and Nelles[16]. In these experiments, air and water flow through a duct consisting of a vertical riser followed by a 90° elbow and finally a horizontal section. Volume fraction profiles were measured at various stations.

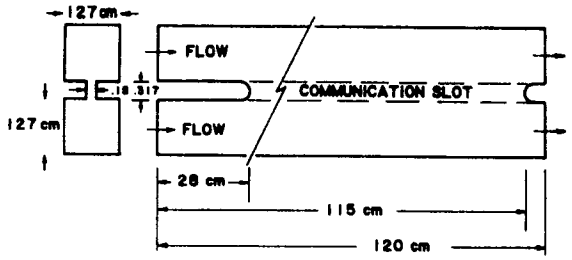

(a) Geometry of the Tapucu experiment subchannels

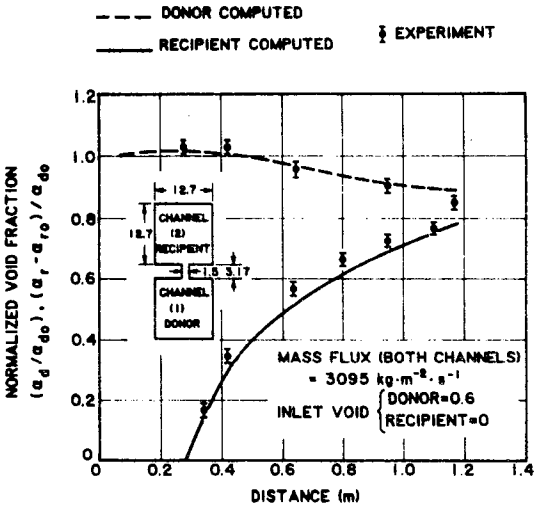

(b) Computed and measured profiles void fraction for horizontal case H_D^R-1

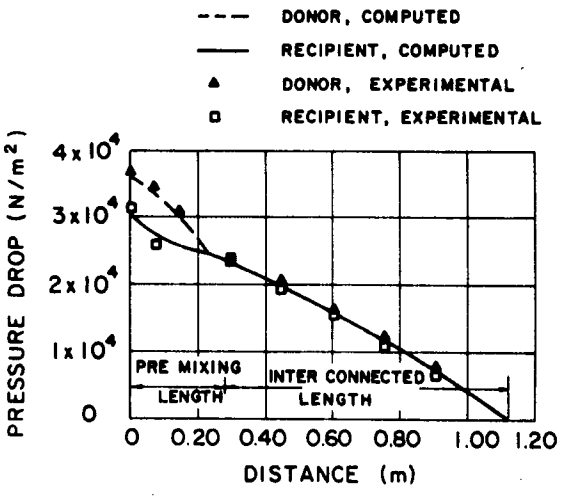

(c) Typical experimental and computed pressure profiles, in this case for test V-1

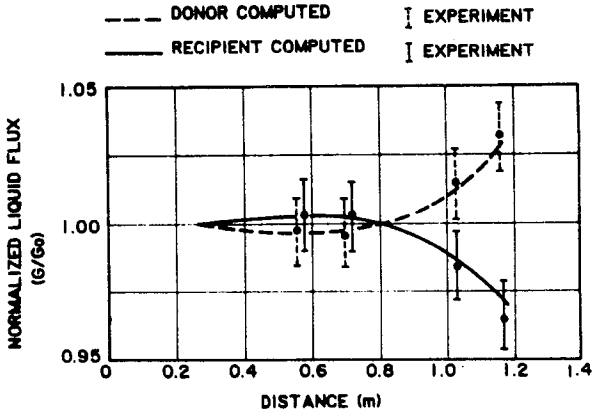

(d) Computed and measured profiles of liquid mass flux for horizontal case H_D^R-1

Figure 7. Simulation of Tapucu Experiments with the ASSERT Code

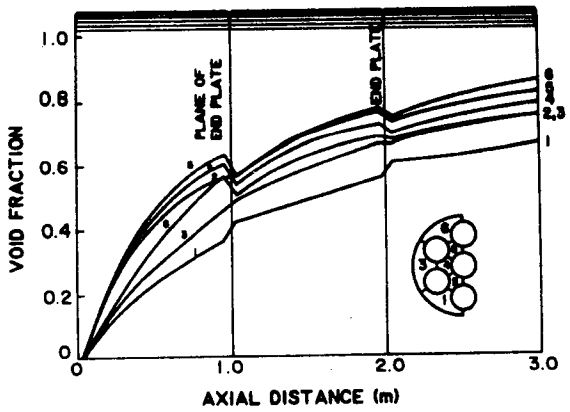

Figure 8. Two-Phase Flow in Hypothetical Horizontal Bundle Simulated by ASSERT

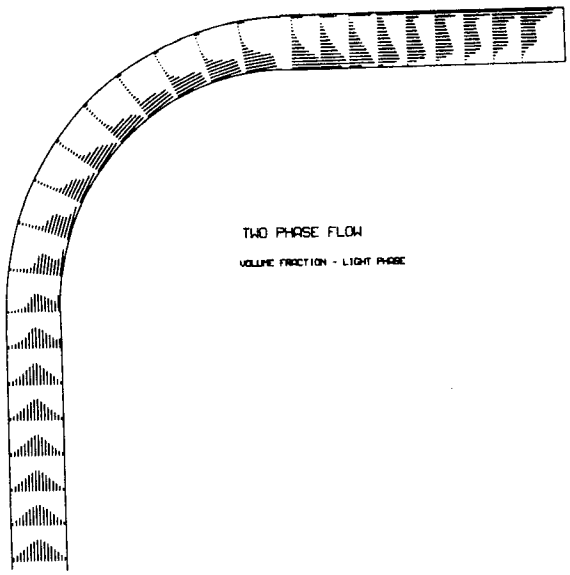

Figure 9. Two Fluid Flow in a Vertical Elbow Air Volume Fraction Computed by TOFFEA

TABLE 3

CONSERVATION EQUATIONS OF ADIABATIC TWO-DIMENSIONAL TWO-FLUID FLOW

Continuity

$$\frac{1}{r}\left[\frac{\partial}{\partial r}(r\rho\alpha v)+\frac{\partial}{\partial\theta}(\rho\alpha u)\right]_i = S\rho_i = -S\rho_j = 0 \qquad \ldots (1)$$

Momentum

θ direction

$$\frac{1}{r}\left[\frac{\partial}{\partial r}(r\rho\alpha uv)+\frac{\partial}{\partial\theta}(\rho\alpha v^2)\right]_i = -\frac{\alpha_i}{r}\frac{\partial P}{\partial\theta}+\rho_i\alpha_i\left[g_\theta+\frac{uv}{r}\right] + \phi_{ij}^{*}(u_j-u_i)+\Gamma_{\theta i}^{*} \qquad \ldots (2a)$$

r direction

$$\frac{1}{r}\left[\frac{\partial}{\partial r}(r\rho\alpha v^2)+\frac{\partial}{\partial\theta}(\rho\alpha uv)\right]_i = -\alpha_i\frac{\partial P}{\partial r}+\rho_i\alpha_i\left[g_r+\frac{u^2}{r}\right]_i + \phi_{ij}^{*}(v_j-v_i)+\Gamma_{ri}^{*} \qquad \ldots (2b)$$

The equations are written for fluid i, analogous equations are written for fluid j.

The equations are converted to cartesian form by substituting

$r = 1$, $\frac{\partial}{\partial r} = \frac{\partial}{\partial y}$, $\frac{\partial}{\partial\theta} = \frac{\partial}{\partial x}$, and omitting the coriolis and centrifugal terms.

α is volume fraction, ρ is density, P pressure, u and v are velocity components, Γ denotes viscous and frictional terms and g is gravitational acceleration.

ϕ is interphase drag function.

*Denotes that constitutive relationships are required for closure.

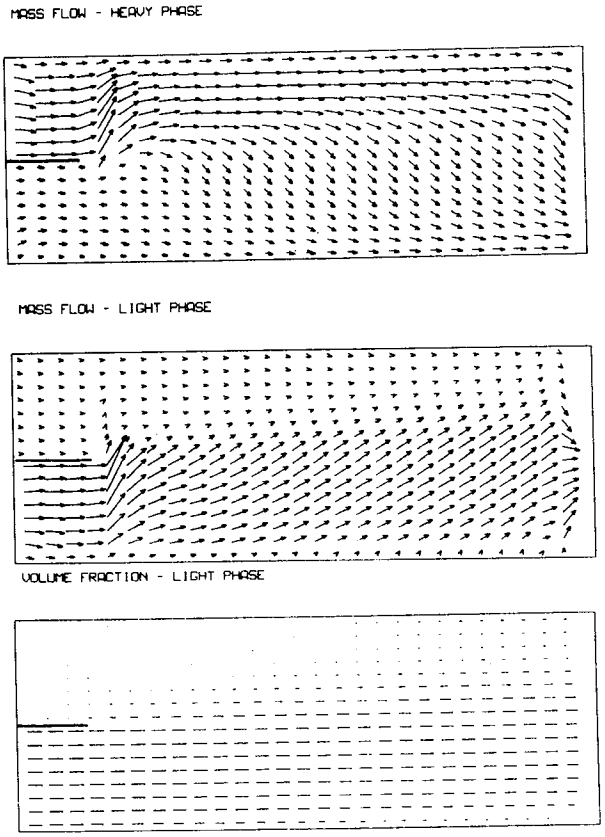

Figure 10. Two Fluid Simulation of Tapucu Experiment by TOFFEA

Computed results for the Gardner and Nelles conditions are shown in Figure 9 in the form of bar graphs depicting radial air volume fraction profiles at various axial stations. Initially in the elbow, the centrifugal force drives the heavier water toward the outer radius and the air inward. Eventually, however, the gravity term dominates and the fluids return to the opposite walls. This switchover makes the simulation numerically difficult, particularly as zero or unit local volume fractions are generated at various points in the profiles. However, continuity is maintained throughout. Quantitative experimental comparisons are given in reference 15.

The TOFFEA code has also been applied to the Tapucu experiments. The final example shows computed distributions of water mass flux, air mass flux and volume profile. Note that the observed switch from co-current to counter-current cross flow is also computed by the two-fluid model.

8.0 CONSTITUTIVE RELATIONSHIPS

Although the calculation procedures have been reviewed and applications illustrated, the next most important ingredients in a thermalhydraulic code are the constitutive relationships required for closure. These are the models of the sub-processes which supply the algebraic relationships necessary for closure, in other words, to balance the number of definitive equations with the number of variables.

In single-phase flow, detailed expressions are required for friction and heat transfer and elements of the turbulence model. In two-phase flow, depending on the model, correlations are needed for void fraction, relative velocity, heat transfer and friction between hardware and each phase and between phases, and the question of flow regime affects all these.

Once a numerical scheme has been developed and exhibited convergence and consistence, the choice of the constitutive relationships determines the detailed results. These must obviously be chosen judiciously. A fairly satisfactory repertoire of relationships has been developed for the homogeneous model. Some doubt exists about the correct choice for the advanced models and further research is continuing.

9.0 VALIDATION

Validation of code predictions against experimental evidence is essential to establish credibility. In order to illustrate that validation is a priority, the figures have been chosento illustrate comparisons with data wherever possible.

10.0 OTHER SOURCES

Multidimensional modelling of single- and homogeneous two-phase flows is quite widespread. However, there are very few reported efforts in the advanced two-phase models. The PHOENICS code of Spalding[17] should be mentioned, as should the Los Alamos TRAC[18]. However, most of the published uses of TRAC appear to be restricted to 1D. The work at Jaycor on steam separation[19], and COBRA-TF[20] both incorporate two-fluid models, the latter also allowing for an entrained substance.

11.0 CONCLUSION

Computational frameworks suitable for multidimensional analyses of both single- and two-phase flow have been reviewed. It is apparent that a common approach is the basis for all cases. It is intended to direct future work in this area towards developing a uniform framework for multidimensional analysis which will be applicable to all the models reviewed. The equations and hence the solution scheme can be written to reduce from the full two-fluid model, successively through the advanced drift model, the basic drift flux model, homogeneous model and hence single-phase flow.

REFERENCES

1. Schlicting, H., Boundary Layer Theory, McGraw-Hill, New York, 1968.

2. Roache, P.S., Computational Fluid Dynamics, Hermosa, Albuquerque, 1976.

3. Sha, W.T., An Overview of Rod-Bundle Thermal-Hydraulic Analysis, Nucl. Eng. & Des., 62, 1980, p.1-24.

4. Domanus, H.M., Sha, V.L. and Sha, W.T., "Applications of the COMMIX Code Using the Porous Medium Formulation," Nucl. Eng. & Des., 62, 1980, p.25-35.

5. Harlow, F.H. and Amsden, A.A., "A Numerical Fluid Dynamics Method for All Speeds," J. Comp. Phys., 8, 1971, p.197-206.

6. Patankar, S.V. and Spalding, D.B., "A Calculation Procedure for Heat Mass and Momentum Transfer in Three Dimensonal Parabolic Flows, Int. J. Heat & Mass Trans., 15, 1972, p.1787-1801.

7. Patankar, S.V., Numerical Heat Transfer and Fluid Flow, Hemisphere, New York, 1980.

8. Carlucci, L.N., "Numerical Simulation of Moderator Flow and Temperature Distribution in a CANDU Reactor Vessel," Int. Symposium on Refined Modelling of Flow, Paris, 1982.

9. Midvidy, W.I. and Austman, H.G., "A 3D Transient Code Used in Thermal Hydraulic Analysis of CANDU Power Reactors, Proceedings 10th IMACS World Congress, Montreal, 1982.

10. Carver, M.B., Carlucci, L.N. and Inch, W.W.R., "Thermalhydraulics in Recirculating Steam Generators, THIRST Code User's Manual," Atomic Energy of Canada Limited report AECL-7254, 1981.

11. Tahir, A. and Carver, M.B., "Numerical Analysis of Two-Phase Flow in Horizontal Channels. SAGA III Code User's Guide," Atomic Energy of Canada Limited report AECL-7613, 1982.

12. Tapucu, A. and Gençay, S., "Experimental Investigation of Mass Exchangers Between Two Laterally Interconnected Two-Phase Flows, École Polytechnique de Montréal, CDT Project No. P-533, 1980.

13. Rowe, D.S., "COBRA-IIIC, A Digital Computer Program for Steady State and Transient Thermalhydraulic Analysis of Rod Bundle Nuclear Fuel Elements," BNWL-1695, 1973.

14. Carver, M.B., Tahir, A., Rowe, D.S., Tapucu, A. and Ahmad, S.Y., "Computational Analyses of Two-Phase Flow in Horizontal Rod Bundles," in press Nucl. Eng. & Des., 1982.

15. Carver, M.B., "Numerical Computation of Phase Separation in Two Fluid Flow," ASME paper 82-FE-2, 1982.

16. Gardner, G.C. and Nelles, P.H., "Phase Distribution in Flow of an Air Water Mixture Round Bends," Proc. Inst. Mech. Engr., 184, Pt. 3C, p.93-101, 1970.

17. Spalding, D.B., "Mathematical Methods in Nuclear Reactor Thermal-Hydraulics," Proceedings of ANS Meeting on Nuclear Reactor Thermal-Hydraulics, Saratoga, N.Y., 1980, R.T. Lahey, editor, P.1979-2023.

18. Liles, D.R., "The Three Dimensional Two Fluid Numerical Treatment of a Reactor Vessel in TRAC," Proceedings of ANS Meeting on Computational Methods in Nuclear Engineering, Williamsburg, 1979, p.1-33, also TRACP1: An Advanced Best Estimate Computer Program for PWR LOCA Analyses, LASL Report NURGE/CR-0063, LA-7279 MSV1, 1978.

19. Stuhmiller, J.H. et al., Numerical Considerations in Multidimensional Two Fluid Calculations, Advances in Computer Methods for Partial Differential Equations, IV, R. Vichnevetsky, editor, IMACS Press, 1981, p.325-331.

20. Kelly, J.M., "Quench Front Modelling and Reflood Heat Transfer in COBRA-TF," ASME paper 79-WA/HT-63, 1979.